Carbohydrate Polymers 87 (2012) 676–686

Contents lists available at SciVerse ScienceDirect

Carbohydrate Polymers

journal homepage: www.elsevier.com/locate/carbpol

Mechanical and water barrier properties of starch/PVA composite films by adding nano-sized poly(methyl methacrylate-*co*-acrylamide) particles

Soon-Do Yoon, Mi-Hwa Park, Hun-Soo Byun*

School of Biotechnology and Chemical System Engineering, Chonnam National University, Yeosu, Jeonnam 550-749, South Korea

ARTICLE INFO

Article history:
Received 19 July 2011
Received in revised form 13 August 2011
Accepted 17 August 2011
Available online 24 August 2011

Keywords:
Starch/PVA composite films
Nano-sized PMMA-*co*-AAm particle
Mechanical properties
Water barrier properties
Biodegradability

ABSTRACT

The aim of this work is to prepare starch/PVA composite films added nano-sized poly(methyl methacrylate-*co*-acrylamide) (PMMA-*co*-AAm) particles and to investigate the mechanical properties, water barrier properties, and soil burial degradation for the films. Composite films were prepared by using corn starch, polyvinyl alcohol (PVA), nano-sized PMMA-*co*-AAm particles, and additives, i.e., glycerol (GL), xylitol (XL), and citric acid (CA). Nano-sized PMMA-*co*-AAm particles were synthesized by emulsion polymerization. The results of the evaluation of properties for prepared films indicated that compared with films without PMMA-*co*-AAm particles, the mechanical properties and water resistance were improved up to 70–400% by the addition of nano-sized PMMA-*co*-AAm. In addition, the results of the soil burial biodegradation revealed that films added PMMA-*co*-AAm particles were degraded by about 45–65% after 165 days.

1. Introduction

Over the past two decades, synthetic polymer materials have been widely used in every field of human activity. These polymers, i.e., polyethylene (PE), polypropylene (PP), polyethylene terephthalate (PET), polystyrene (PS), and polycarbonate (PC), are usually petroleum based and are regarded as non-degradable. However, since the petroleum resources are limited and the increasing use of non-biodegradable polymers has caused serious environmental problems, degradable and/or biodegradable polymer materials have been attracting an increasing attention since the 1970s (Ahamed, Singhal, Kulkarni, Kale, & Pal, 1996; Koenig & Huang, 1995; Vert et al., 2002). Consequently, there is a growing interest in developing biodegradable polymers made from renewable and natural polymers such as cellulose, starch, and proteins to replace synthetic non-degradable materials (Ishiaku, Pang, Lee, & Ishak, 2002; Mathew & Dufresne, 2002).

Of these materials, starch, the natural polymer, is an inexpensive and readily available resource, which is often used as a filler for the replacement of petroleum derived synthetic polymers to reduce environmental pollution (Psomiadou, Arvanitoyannis, Biliaderis, Ogawa, & Kawasaki, 1997; Yun & Yoon, 2010). However, since thermoplastic starch has limitations in terms of both mechanical properties and water resistance, substantial effort has been made to improve these properties by adding certain synthetic polymers, i.e., starch/polyvinyl alcohol (PVA), starch/poly(lactic acid) (PLA), and starch/polyester blend polymers (Guana, Eskridgeb, & Hannaa, 2005; Huneault & Li, 2007; Liao & Wu, 2009; Ren, Fu, Ren, & Yuan, 2009). Thus, starch/PVA blended films have become one of the most popular biodegradable polymers. However, their physical properties such as mechanical properties and water resistance are still lower than those of other synthetic polymers made from petroleum. Many researchers have attempted to resolve these problems by electron beam and ultraviolet irradiation (Khan, Bhattacharia, Kader, & Bahari, 2006; Zhai, Yoshii, & Kume, 2003), by adding crosslinking agents (Yoon, Chough, & Park, 2007), by using of chemically modified starch (Ma, Jian, Chang, & Yu, 2008; Yun, Wee, Byun, & Yoon, 2008), or by preparing biodegradable nanocomposites polymer adding nanoparticles (Azeredo, 2009; Chivrac, Pollett, & Schmutz, 2008; Jordan, Jacob, Tannenbaum, Sharaf, & Jasiuk, 2005; Yu, Lin, Yeh, & Lin, 2003).

Of these methods, biodegradable nanocomposite polymers have attracted significant scientific attention because of their barrier and mechanical properties. Defined as composite materials for which one of the phases has at least one dimension in the nanometer range (1–100 nm), biodegradable nanocomposite polymers have been prepared using organic–inorganic nanoclay or silicate, and their mechanical properties, water resistance, and thermal properties have been examined. Avella et al. (2005) and Cyras, Manfredi, Ton-That, and Vázquez (2008). These workers have generated starch/clay nanocomposites with improved mechanical properties, and reduced water vapor permeability. Rhim, Hong, and Ha (2009) have reported that physical properties of polylactic acid

* Corresponding author. Tel.: +82 61 659 7296; fax: +82 61 653 3659.
E-mail address: hsbyun@chonnam.ac.kr (H.-S. Byun).

0144-8617/$ – see front matter © 2011 Elsevier Ltd. All rights reserved.
doi:10.1016/j.carbpol.2011.08.046

(PLA) as biodegradable polymers are improved by the addition of nanoclay. Tang, Xiong, Tang, and Zou (2009) have reported that nano-SiO_2 are capable of improving physical properties, i.e., mechanical properties and elongation at break, and water resistance of starch/PVA blended polymers. Other additional advantages have been reported on the performance of polymers as a result of using nanoclay or nano-SiO_2, including increased glass transition and thermal degradation temperatures (Cabedo, Gimenez, Lagaron, Gavara, & Saura, 2004; Chang, An, & Sur, 2003; Lee, Chen, & Hannaa, 2008; Ogata, Jimenez, Kawai, & Ogihara, 1997; Pluta, Galeski, Alexandre, Paul, & Dubois, 2002). Thus, it has been shown that the addition of nano-sized clay or SiO_2 particles for biodegradable polymers improved the physical and thermal properties for their use. However, addition of nanoclay or nano-SiO_2 on biodegradable polymers showed an effect of drastically reducing the elongation and relative slowness of the degree of biodegradation. Moreover, when biodegradable polymers are prepared by the blending and casting method, agglomeration is formed between inorganic nano-materials and polymers. Therefore, to solve the problems of reduced elongation, slow biodegradation, and agglomeration, it is necessary to develop new nano-sized particles.

In this work, we synthesized the starch/PVA composite films from corn starch, PVA, and nano-sized poly(methyl methacrylate-*co*-acrylamide) (PMMA-*co*-AAm) using a casting method, and we also investigated the effect of nano-sized PMMA-*co*-AAm contents, the MMA mole ratio of PMMA-*co*-AAm, and the particle size of nano-sized PMMA-*co*-AAm on physical properties such as tensile strength, elongation at break, degree of swelling, solubility, water vapor absorption, and biodegradation as monitored by a soil burial test

2. Experimental

2.1. Materials

Corn starch was obtained from Doosan Corn Products Korea, Inc. Methyl methacrylate (MMA), acrylamide (AAm, >99%+), potassium persulfate (K2S2O8; KPS), sodium dodecylsulfate (SDS), polyvinyl alcohol (PVA), glycerol (GL), xylitol (XL), and citric acid (CA) were purchased from Aldrich Chemical Company, Inc. (Milwaukee, WI). PVA was 99% hydrolyzed with a molecular weight average of 89,000–98,000. MMA was distilled under vacuum to remove the inhibitors before polymerization. Distilled deionized water (DW) was used in all experiments.

2.2. Preparation of nano-sized PMMA-co-AAm particles

Nano-sized poly(methyl methacrylate-*co*-acrylamide) (PMM-*co*-AAm) particles were synthesized by emulsion copolymerization in a 500 mL reactor at a constant stirring rate of 300 rpm in a nitrogen atmosphere. DW (400 mL), 1.5 wt.% surfactant SDS, 1.0 wt.% KPS as initiator, and monomers (MMA and AAm) were added to the reaction bottle. SDS and KPS are added a mass percent ratio to total MMA and AAm weight. MMA and AAm were added at the difference mole ratio of 1:1 (12.8 g:9.1 g, PMAm11), 2:1 (16.7 g:6.0 g, PMAm21), 3:1 (16.7 g:4.0 g, PMAm31), and 4:1 (18.2 g:3.2 g, PMAm41), respectively. In addition, the PMMA-*co*-AAm added different KPS as initiator (0.25, 0.5, 1.0, and 1.5 wt.%) were synthesized to control the particle sizes. The reaction time and temperature for preparing latex were 20 h and 60 °C. The latex was dialyzed in DW at room temperature for 3 days for characterize and prepare starch/PVA composite blend films. The overall conversion of copolymers was calculated by the method of Veregin, Odell, Michalak, and Georges (1996) using a thermo gravimetry analysis (TGA). The TGA (TGA 851, Metter Toledo) conversion measurement was performed in nitrogen at a heating rate of 10 °C/min from room temperature to 300 °C. The size and the shape were also observed using scanning electron microscopy (SEM, S-4700, Hitachi, Japan).

2.3. Preparation of starch/PVA composite blend films

Starch/PVA composite films were prepared using a casting method. Starch/PVA/PMMA-*co*-AAm composite films were prepared as follows. First, PVA solution was prepared by dissolving PVA in hot water (90 °C). Corn starch (CS), PMMA-*co*-AAm latex containing copolymers of 10, 20, 30, 40, and 50 wt.% and 40 wt.% additives (GL, XL, and CA) were mixed directly together with water using a Kitchen-aid mixer (Anymix, Hyun-woo Star, Seoul, Korea) for 20 min. CS and PVA had the same mass ratio, and the content of PMMA-*co*-AAm and additives was expressed as a mass percent ratio to total CS and PVA weight, respectively. The PVA solution and mixed starch/PMMA-*co*-AAm/additives were mixed at 90 °C for 20 min. Then, the mixture was blended to form a homogeneous gel-like solution with a mechanical stirrer (200 rpm) at room temperature for 80 min. The mixing composition is shown in Table 1. Bubbles, the by-product of preparation, were removed by using an aspirator. Thus, the prepared gel-like solution was poured on to a pre-warmed (50 °C) Teflon mold (200 mm × 200 mm × 1 mm). Water was evaporated from the molds in a ventilated oven at 50 °C for 24 h. Table 2 shows the mixing composition of films added PMMA-*co*-AAm particles which are prepared at the different mole ratio of MMA and AAm and the different particle sizes. Dried films were put in open polyethylene bags and stored at 25 °C and at relative humidity (RH) of 57% for 1 week before they were measured.

2.4. Mechanical properties of films

Tensile strength (TS) and elongation at break (%E) were evaluated for each film using the Instron 6012 testing machine (USA). Five dumbbell shaped specimens (ASTM D-412) were cut out of each film. Each specimen had a width of 12 mm. The average thickness of the specimen was about 0.11 mm. The thickness of the films was measured on a mechanical scanner (Digital thickness gauge 'Mitutoyo' Tokyo, Japan) at 20 random positions around the film. The mean standard deviation within the film was about 5% of the average thickness. The gauge length and grip distance were both 50.0 mm. Crosshead speed was 20 mm/min and load cell was 250 kg_f. The tests were carried out at 23 °C and 55% RH at a constant temperature and humidity room.

2.5. Degree of swelling and solubility of films

The degree of swelling (DS) and solubility (S) of the films were measured applying the following method. Dried biodegradable starch/PVA composite blend films were immersed in distilled water at room temperature (25 °C). After the equilibrium (24 h), moisture on the surface of the film was removed, and the weight of the films was measured. DS in films was calculated as (1):

$$\mathrm{DS} = \frac{(W_e - W_0)}{W_0} \quad (1)$$

where W_e is the weight of the film at the adsorbing equilibrium, and W_0 is the first dry weight of the film.

The swollen films were dried again for 24 h at 60 °C, and its solubility (S) was calculated with the following Eq. (2):

$$S = \frac{(W_0 - W_d)}{W_d} \quad (2)$$

where W_0 is the first dry weight of the film and W_d is the dry weight of the swollen film.

Table 1
Composition of gel-like solutions used to prepare biodegradable composite blend films.

Sample name	CS (g)	PVA (g)	PMAm11 (wt.%)	GL (wt.%)	XL (wt.%)	CA (wt.%)	DW (g)
CSPN0	5	5	–	–	–	–	100
CSPN1	5	5	10	–	–	–	100
CSPN2	5	5	20	–	–	–	100
CSPN3	5	5	30	–	–	–	100
CSPN4	5	5	40	–	–	–	100
CSPN5	5	5	50	–	–	–	100
CSPG4N0	5	5	–	40	–	–	100
CSPG4N1	5	5	10	40	–	–	100
CSPG4N2	5	5	20	40	–	–	100
CSPG4N3	5	5	30	40	–	–	100
CSPG4N4	5	5	40	40	–	–	100
CSPG4N5	5	5	50	40	–	–	100
CSPX4N0	5	5	–	–	40	–	100
CSPX4N1	5	5	10	–	40	–	100
CSPX4N2	5	5	20	–	40	–	100
CSPX4N3	5	5	30	–	40	–	100
CSPX4N4	5	5	40	–	40	–	100
CSPX4N5	5	5	50	–	40	–	100
CSPC4N0	5	5	–	–	–	40	100
CSPC4N1	5	5	10	–	–	40	100
CSPC4N2	5	5	20	–	–	40	100
CSPC4N3	5	5	30	–	–	40	100
CSPC4N4	5	5	40	–	–	40	100
CSPC4N5	5	5	50	–	–	40	100

2.6. Water vapor absorption

The pieces of prepared films were cut into small pieces (5 cm × 5 cm) and the weight of pieces was measured immediately. Then, they were dried in an oven at 60 °C overnight and weighed. The water content (k) of starch/PVA composite films was calculated as (3):

$$k = \frac{(W_f - W_0)}{W_0} \quad (3)$$

where W_0 is the mass of the dried sample and W_f is the mass of the sample before drying. Water vapor adsorption of the films was evaluated after storage in desiccator chambers over the salt solutions at constant 51% RH for 10 days at 25 °C. Constant 51% RH was obtained with saturated salt solutions of $Ca(NO_3)_2\,4H_2O$ (~51% relative humidity).

2.7. Soil burial degradation test

The soil burial degradation was carried out as described by Thakore, Desai, Sarawade, and Devi (2001). Garden pots with an approximate capacity of 10 L were filled with soil taken from a culture field in Naju City (Korea). The plastic samples were cut into 3 cm × 3 cm pieces and buried in the soil at the depth of 10 cm. The

Table 2
Composition of gel-like solutions used to prepare biodegradable composite films in terms of methyl methacrylate contents (mole) and the particle size of PMMA-*co*-AAm.

Sample name	PMAm21 (wt.%)	PMAm31 (wt.%)	PMAm41 (wt.%)	PMMA (wt.%)	PMAm4160 (wt.%)	PMAm41150 (wt.%)	PMAm41200 (wt.%)	DW (g)
CSPN213	30	–	–	–	–	–	–	100
CSPN313	–	30	–	–	–	–	–	100
CSPN413	–	–	30	–	–	–	–	100
CSPG4N213	30	–	–	–	–	–	–	100
CSPG4N313	–	30	–	–	–	–	–	100
CSPG4N413	–	–	30	–	–	–	–	100
CSPX4N213	30	–	–	–	–	–	–	100
CSPX4N313	–	30	–	–	–	–	–	100
CSPX4N413	–	–	30	–	–	–	–	100
CSPC4N213	30	–	–	–	–	–	–	100
CSPC4N313	–	30	–	–	–	–	–	100
CSPC4N413	–	–	30	–	–	–	–	100
CSPNP3	–	–	–	30	–	–	–	100
CSPG4NP3	–	–	–	30	–	–	–	100
CSPX4NP3	–	–	–	30	–	–	–	100
CSPC4NP3	–	–	–	30	–	–	–	100
CSPN41-1	–	–	–	–	30	–	–	100
CSPN41-2	–	–	–	–	–	30	–	100
CSPN41-3	–	–	–	–	–	–	30	100
CSPG4N41-1	–	–	–	–	30	–	–	100
CSPG4N41-2	–	–	–	–	–	30	–	100
CSPG4N41-3	–	–	–	–	–	–	30	100
CSPX4N41-1	–	–	–	–	30	–	–	100
CSPX4N41-2	–	–	–	–	–	30	–	100
CSPX4N41-3	–	–	–	–	–	–	30	100
CSPC4N41-1	–	–	–	–	30	–	–	100
CSPC4N41-2	–	–	–	–	–	30	–	100
CSPC4N41-3	–	–	–	–	–	–	30	100

[a] Corn starch and PVA were added to 5 g as the same mass ratio, and additives (GL, XL, and CA) were added 40 wt.% as mass percent ratio to total CS and PVA weight, respectively.

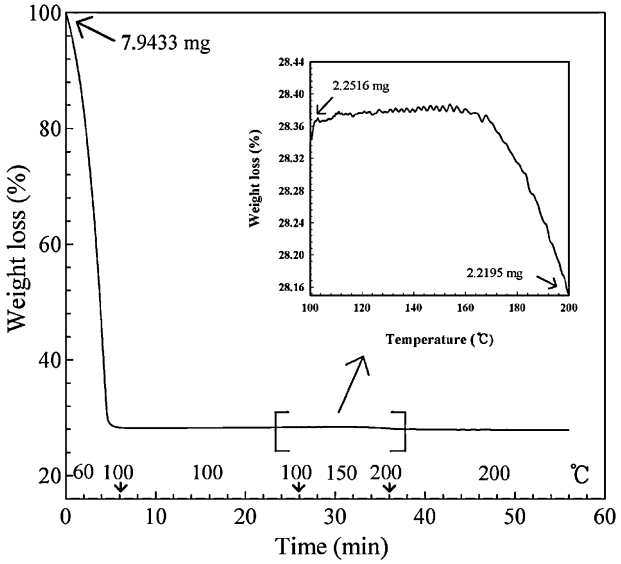

Fig. 1. Thermo gravimetry analysis (TGA) curve of nano-sized PMMA-*co*-AAm prepared at the same mole ratio of MMA and AAm.

pots were placed in an uncovered gazebo. The soil was kept moist by sprinkling water at a regular time interval to maintain 30–50% humidity. The excess water was drained through the hole at the bottom of the pot. The degradation of the specimen was determined at a regular time interval (15 days) by taking the specimen carefully from the soil and washing it gently with distilled water to remove the soil. The specimen was dried in an oven until a constant weight was obtained. Weight loss of the specimen with time was used to indicate the degradation rate in the soil burial test. The soil burial degradation test started on May 15, 2009 and ended on November 15, 2009.

3. Results and discussion

3.1. Characterization of nano-sized PMMA-co-AAm

The conversion of nano-sized PMMA-*co*-AAm was analyzed by using the thermo gravimetry analysis (TGA) method reported by Veregin et al. The conversion rate is calculated by comparing the weight loss caused by the vaporization of monomer during polymer decomposition. The TGA conversion measurement was performed at a heating rate of 10 °C/min and starting from room temperature up to 300 °C under nitrogen. There was a clear plateau in the weight loss data up to 200 °C, at which point the monomer has volatilized, and polymer degradation began at 300 °C. Thus, the weight loss below about 200 °C represents the monomer content, while the weight loss above about 300 °C expresses the polymer content. As shown in Fig. 1, the dispersion medium, i.e., distilled deionized water inside the synthesized nano-sized PMMA-*co*-AAm (1:1) latex was evaporated at 100 °C, and the synthesized PMMA-*co*-AAm and unreacted monomers remained. The unreacted monomers and oligomers are either evaporated or decomposed between 100 °C and 200 °C because the boiling points of MMA and AAm that were used as monomer are 115 °C and 125 °C, respectively. If follows, therefore, that synthesized polymer particles are decomposed above 250 °C. Therefore, the conversion was calculated by the ratio of the residual quantity after evaporation dispersion medium and the residual quantity at 200 °C. As a result, the conversion was about 99.0%.

Fig. 2 represents the SEM images of nano-sized PMMA-*co*-AAm prepared by the different mole ratio of MMA and AAm. The images show that nano-sized PMMA-*co*-AAm particles are successfully prepared. In addition, the agglomeration between particles was observed because the greater the decrease in the MMA mole ratio, the greater the increase in the hydrophilic properties. The surface of their particles was smooth and had a regular spherical shape except for PMAm11. The average size of spherical copolymer particles was about 100 nm.

To investigate the effect of particle sizes of PMMA-*co*-AAm for starch/PVA composite films, PMMA-*co*-AAm (4:1) was synthesized whose particle size was controlled by the changing the initiator concentration. In general, the particle sizes are controlled through reaction temperature, monomer concentration, initiator density, steric stabilizer concentration, and medium solvency. Thus, in this study, PMMA-*co*-AAm particles were synthesized whose sizes are different from each other by changing the initiator concentration (0.25, 0.5, 1.0, and 1.5 wt.%) (Fig. 2(f)–(h)). The particle sizes increased in accordance with the decrease in the initiator (KPS) concentration at the same condition, i.e., temperature, rpm, surfactant content (SDS), and solvency of medium (DW). The surface was mostly smooth and had a regular spherical shape. The particle sizes were about 60, 100, 150, and 200 nm, respectively.

3.2. Mechanical properties of films

Fig. 3(a) and (b) represents the results of tensile strength (TS) and elongation at break (%E) for films with nano-sized PMMA-*co*-AAm particles contents. Nano-sized PMMA-*co*-AAm particles which were prepared at the same mole ratio of MMA and AAm were used and 40 wt.% (corn starch and PVA weight bases) GL, XL, and CA as additives are added, respectively. With the increase of the PMMA-*co*-AAm particles contents (10–50 wt.%), TS increased whereas %E decreased compared with that of films without added particles. For example, TS increased about 60.0% (none additive), 413.9% (GL-added film). 380.1% (XL-added film), and 148.0% (CA-added film); conversely %E decreased about 420.5% (none additive), 148.2% (GL-added film), 110.3% (XL-added film), and 151.9% (CA-added film) when nano-sized PMMA-*co*-AAm particles contents increased from 0 to 50 wt.%. In addition, as previously reported work (Yoon, Chough, & Park, 2006), the results of TS and %E with additives verified that the film to which CA with hydroxyl and carboxyl groups was added is stronger and more flexible than the film to which GL and XL with hydroxyl group was added. Comparison of the GL (with 3 hydroxyl group) added film with the XL (with 5 hydroxyl group) added films showed that TS and %E of XL-added film were higher than those of the GL-added film. In addition, Fig. 3(c) and (d) represents the results of TS and %E for the films added with different size PMMA-*co*-AAm particles. The PMMA-*co*-AAm particles were prepared at the mole ratio of 4:1 (MMA:AAm) and particle sizes were controlled by changing initiator contents (0.25, 0.5, 1.0, and 1.5 wt.%). TS value increased until the size of added nanoparticles reached 150 nm and it decreased when the size of added nanoparticles grew bigger than 150 nm whereas %E drastically decreased. A possible explanation of this phenomenon is that when different size PMMA-*co*-AAm particles are added to starch/PVA/additives mixture, the inter–intramolecular interfacial adhesion is weakened as the added particle size increases in the composite film because the interaction between PMMA-*co*-AAm and starch or between PMMA-*co*-AAm and PVA is hindered.

Fig. 4 shows the SEM micrographs of the surface of films to which 30 wt.% PAAM-*co*-AAm particle and additives are added, respectively. It is possible to see a very good dispersion of PAAM-*co*-AAm nanoparticle for films, as there is no rough areas or large agglomerates.

In order to investigate the effect of copolymer nanoparticles with hydrophobic and hydrophilic, PMMA-*co*-AAm nanoparticles were synthesized by the increase of MMA mole ratio, then films added copolymer nanoparticles with the different mole ratio of

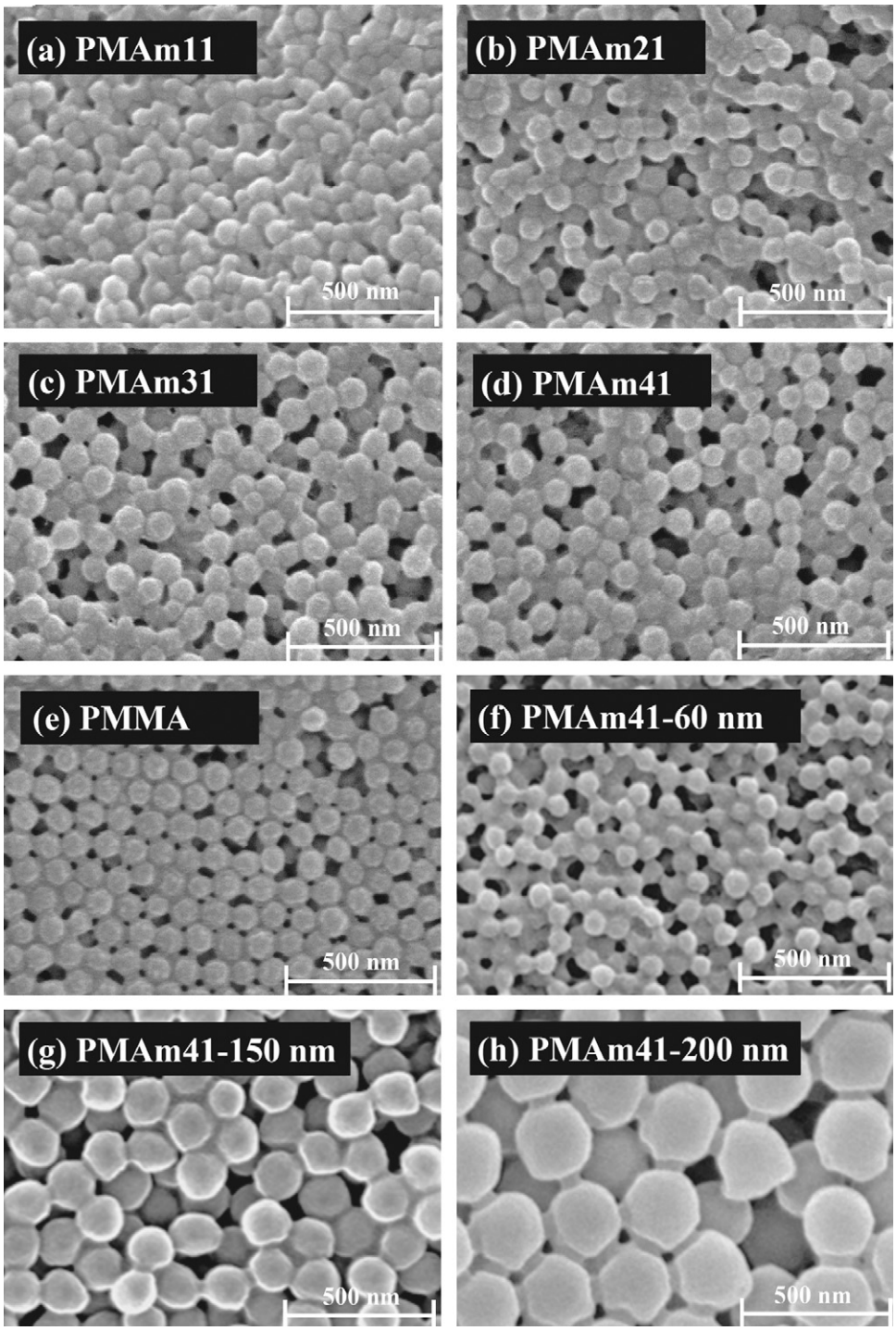

Fig. 2. SEM image of nano-sized PMMA-*co*-AAm particles synthesized by the different mole ratio of MMA and AAm and the PMAm41 particles prepared at various KPS. (a) SEM image of PMAm11 prepared at the same mole ratio of MMA and AAm (1:1). (b) SEM image of PMAm21 prepared at the mole ratio of MMA and AAm (2:1). (c) SEM image of PMAm31 prepared at the mole ratio of MMA and AAm (3:1). (d) SEM image of PMAm41 prepared at the mole ratio of MMA and AAm (4:1). (e) SEM image of PMMA. (f) SEM image of PMAm41 added 1.5 wt.%. KPS. (g) SEM image of PMAm41 added 0.5 wt.%. KPS. (h) SEM image of PMAm41 added 0.25 wt.%. KPS.

MMA and AAm were evaluated for their TS and %E. Table 3 represent the results of TS and %E of the films added PMMA-*co*-AAm nanoparticles prepared by the change of MMA mole ratio. With increasing MMA mole ratio with hydrophobic property, TS values slightly increased whereas %E decreased rapidly. In addition, the films added PMMA nanoparticles without hydrophilic property were too brittle due to the absence of the functional group which can combine between starch, PVA and additives with hydrophilic property when compared to those of the addition of copolymer nanoparticles with hydrophobic and hydrophilic properties.

3.3. Degree of swelling and solubility of films

The measurement of swelling and solubility for the films plays a key role in determining the degree of combination between the components of films as well as resistance to water (Anglès &

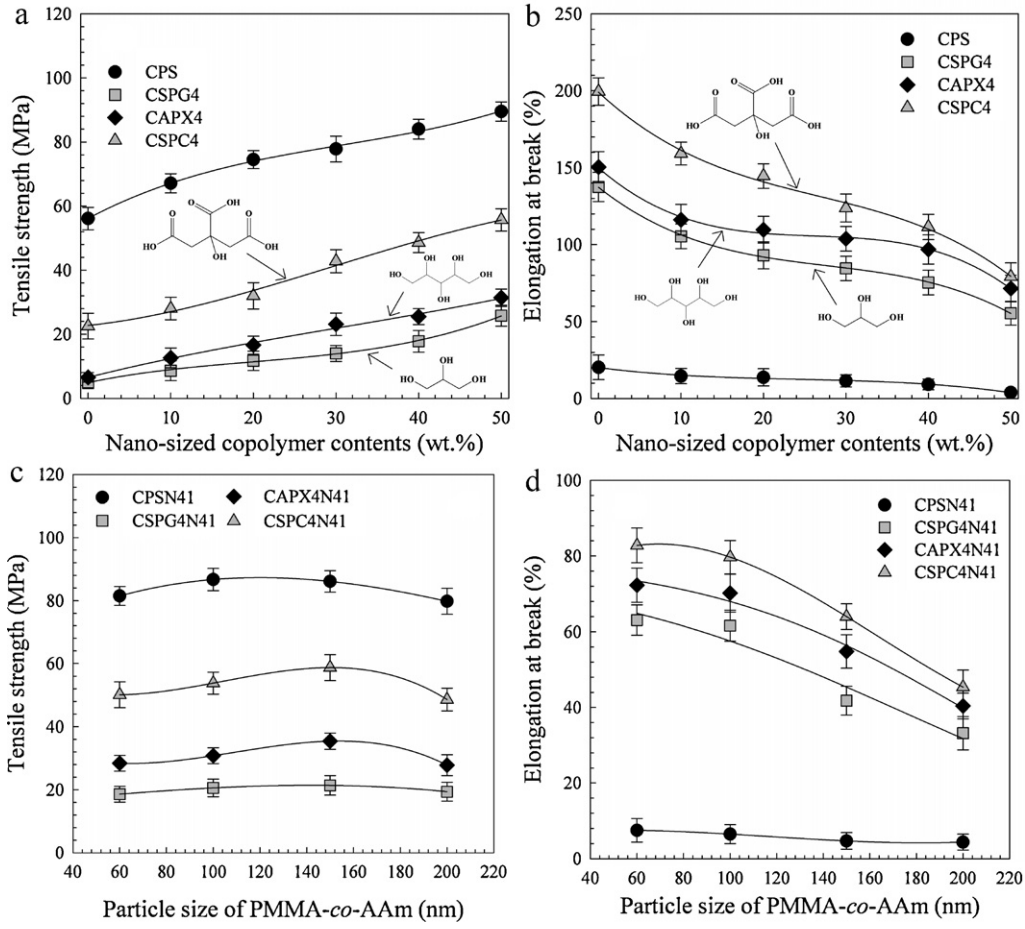

Fig. 3. Tensile strength (TS) and elongation at break (%E) of starch/PVA composite films in terms of PMAm11 nanoparticles contents and added with different particle size of PMAm41. (a) TS of starch/PVA composite films in terms of PMAm11 nanoparticles contents. (b) %E of starch/PVA composite films in terms of PMAm11 nanoparticles contents. (c) TS of starch/PVA composite films added with different particle size of PMAm41. (d) %E of starch/PVA composite films added with different particle size of PMAm41.

Dufresne, 2000; Mathew, Brahmakumar, & Abraham, 2006). The degree of swelling (DS) and solubility (*S*) of starch/PVA composite films with PMMA-*co*-AAm contents prepared at the same mole ratio of MMA and AAm are shown in Fig. 5(a) and (b). As the PMMA-*co*-AAm nanoparticles contents increased, DS value increased whereas *S* value decreased. This result illustrates that inter–intramolecular combination is improved by the presence of interactions between the added nano-sized PMMA-*co*-AAm and the starch/PVA/additives mixture. Although each film has different additives, the water resistance of each film was improved by the addition of PMMA-*co*-AM

Table 3
Tensile strength, elongation at break, degree of swelling, and solubility of starch/PVA composite films in terms of methyl methacrylate contents (mole) of nano-sized PMMA-*co*-AAm.

Sample name	Tensile strength (MPa)	Elongation at break (%)	Degree of swelling (g/g)	Solubility (g/g)
CSPN113	77.8 ± 4.0	11.5 ± 3.5	2.777 ± 0.090	0.155 ± 0.019
CSPN213	82.0 ± 3.9	7.8 ± 2.5	2.881 ± 0.099	0.141 ± 0.020
CSPN313	84.6 ± 4.1	7.3 ± 2.4	2.925 ± 0.085	0.137 ± 0.015
CSPN413	86.7 ± 3.6	6.5 ± 2.5	2.994 ± 0.120	0.126 ± 0.013
CSPG4N113	13.9 ± 2.5	84.6 ± 5.1	1.198 ± 0.091	0.536 ± 0.018
CSPG4N213	18.5 ± 3.1	77.1 ± 6.0	1.287 ± 0.087	0.519 ± 0.019
CSPG4N313	19.4 ± 3.5	68.5 ± 4.1	1.294 ± 0.095	0.506 ± 0.030
CSPG4N413	20.6 ± 3.4	61.6 ± 3.9	1.344 ± 0.100	0.491 ± 0.015
CSPX4N113	23.1 ± 3.1	103.8 ± 7.5	1.383 ± 0.110	0.474 ± 0.019
CSPX4N213	27.7 ± 3.5	90.5 ± 6.4	1.509 ± 0.098	0.452 ± 0.017
CSPX4N313	28.9 ± 3.4	86.6 ± 5.5	1.574 ± 0.087	0.441 ± 0.021
CSPX4N413	30.8 ± 4.0	70.2 ± 6.4	1.663 ± 0.075	0.426 ± 0.014
CSPC4N113	42.8 ± 3.0	123.8 ± 7.0	2.421 ± 0.079	0.375 ± 0.018
CSPC4N213	48.0 ± 2.5	103.0 ± 6.8	2.522 ± 0.098	0.353 ± 0.022
CSPC4N313	49.8 ± 4.1	95.6 ± 6.5	2.569 ± 0.099	0.348 ± 0.015
CSPC4N413	53.8 ± 3.2	79.7 ± 5.8	2.641 ± 0.100	0.327 ± 0.011
CSPNP3	95.8 ± 4.0	5.6 ± 2.3	2.432 ± 0.088	0.231 ± 0.020
CSPG4NP3	35.8 ± 4.2	40.1 ± 3.0	1.017 ± 0.120	0.592 ± 0.021
CSPX4NP3	49.1 ± 3.4	44.8 ± 2.9	1.119 ± 0.105	0.501 ± 0.015
CSPC4NP3	68.3 ± 4.1	53.7 ± 4.5	2.001 ± 0.089	0.395 ± 0.016

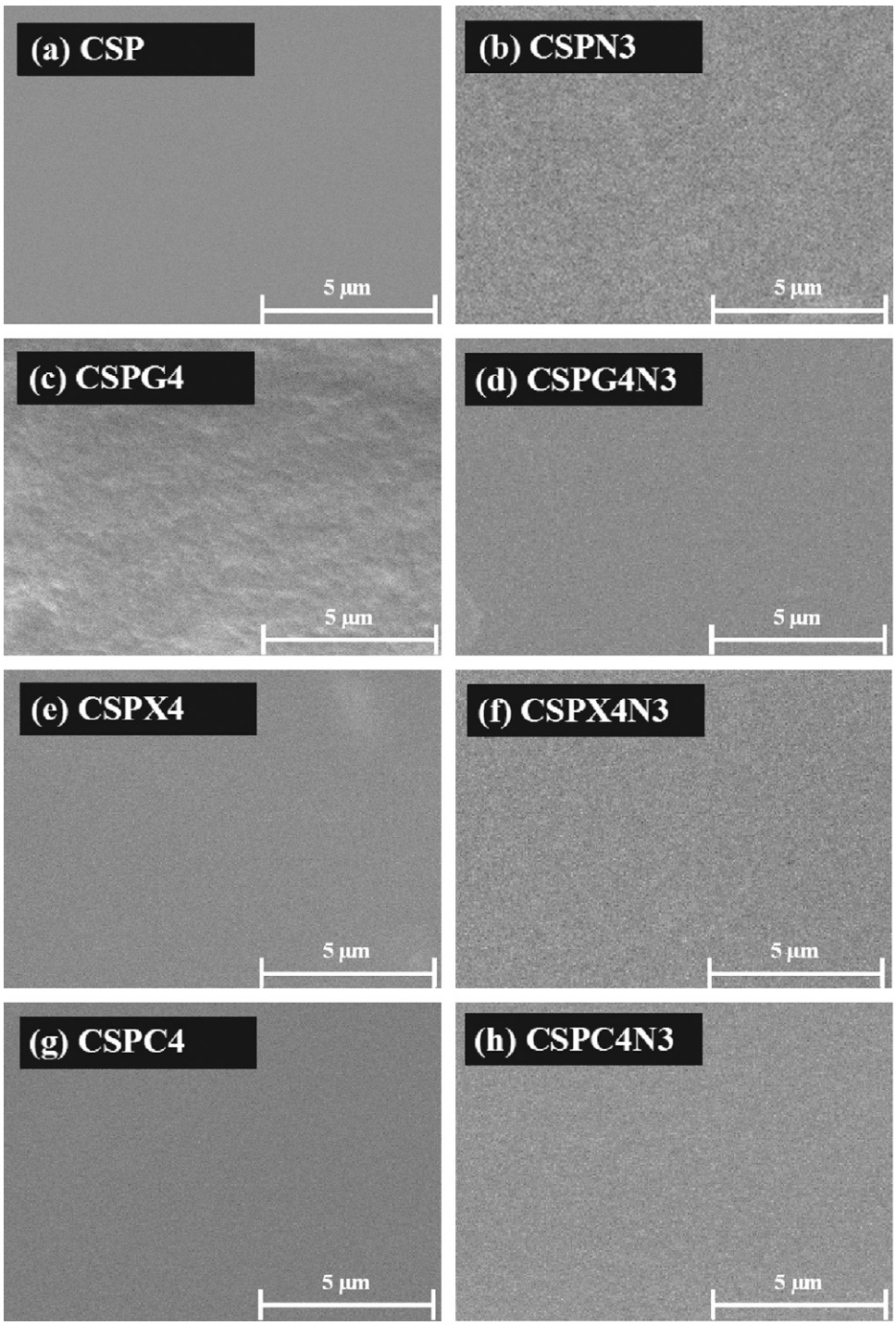

Fig. 4. Scanning electron microscope (SEM) image of the surface of starch/PVA composite films with/without added the PMAm11 nanoparticles. (a) Film without added additive and PMAm11 nanoparticles. (b) Film without added additive and containing 30 wt.% PMAm11 nanoparticles. (c) Film added 40 wt.% GL. (d) Film containing 40 wt.% GL and 30 wt.% PMAm11 nanoparticles. (e) Film added 40 wt.% XL. (f) Film containing 40 wt.% XL and 30 wt.% PMAm11 nanoparticles. (g) Film added 40 wt.% CA. (h) Film containing 40 wt.% CA and 30 wt.% PMAm11 nanoparticles.

nanoparticles. In addition, we found that the water resistance of the synthesized films was superior to that of the other films prepared using added nanoclay (Cyras et al., 2008; Dean, Yu, & Wu, 2007; Park, Lee, Park, Cho, & Ha, 2003) or nano-SiO_2 particles (Tang, Zou, Xiong, & Tang, 2008; Xiong, Tang, Tang, & Zou, 2008).

Fig. 5(c) and (d) shows the results of DS and *S* of films added with the different particle size PMMA-*co*-AAm (60, 100, 150, and 200 nm). As the particle size of PMMA-*co*-AAm increase, DS values drastically decreased and *S* values were increased. In other words, the increase in particle size led to a decrease in water resistance for the films. It was confirmed that voids which can absorb H_2O molecules are generated as the particle size increased and agglomerations take place between particles in the composite films. To verify this phenomenon, SEM images of the films were investigated. Fig. 6 clearly demonstrates that as the particle size of PMMA-*co*-AAm added to films increases, agglomerations and phase separation occur on the film surface. In addition, these phenomena cause the deterioration of the overall physical properties.

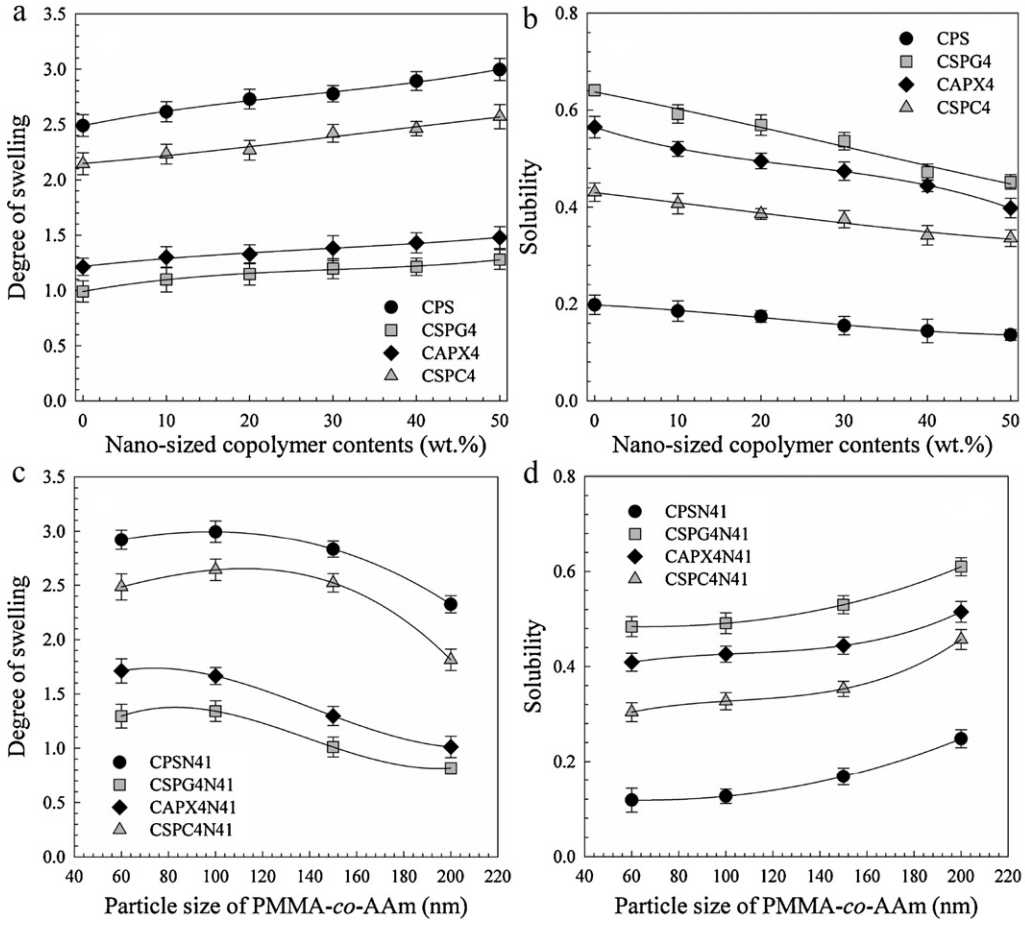

Fig. 5. Degree of swelling (DS) and solubility (*S*) of starch/PVA composite films in terms of PMMA-*co*-AAm contents and films added with different particle size of PMAm41. (a) DS of starch/PVA composite films in terms of PMMA-*co*-AAm contents. (b) *S* of starch/PVA composite films in terms of PMMA-*co*-AAm contents. (c) DS of starch/PVA composite films added with different particle size of PMAm41. (d) *S* of starch/PVA composite films added with different particle size of PMAm41.

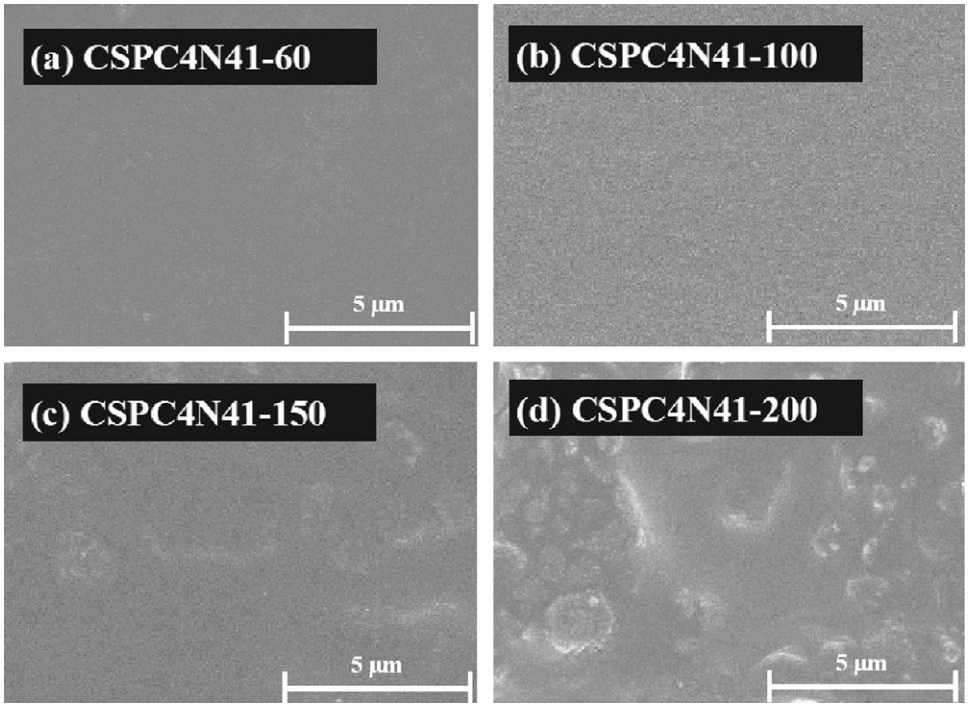

Fig. 6. Scanning electron microscope (SEM) image of the surface of starch/PVA composite films added with different particle size of PMAm41. (a) Film containing 40 wt.% CA and 30 wt.% PMAm41 nanoparticles (60 nm). (b) Film containing 40 wt.% CA and 30 wt.% PMAm41 nanoparticles (100 nm). (c) Film containing 40 wt.% CA and 30 wt.% PMAm41 nanoparticles (150 nm). (d) Film containing 40 wt.% CA and 30 wt.% PMAm41 nanoparticles (200 nm).

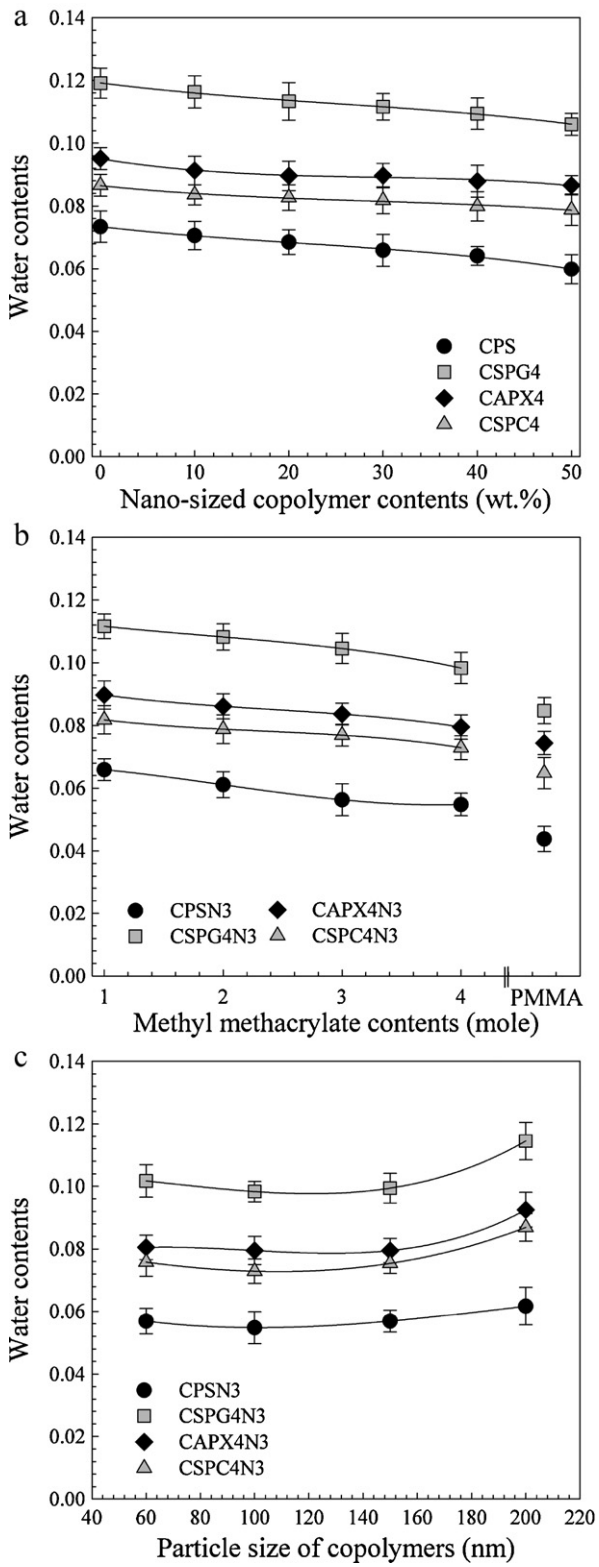

Fig. 7. Water contents of prepared starch/PVA composite films. (a) Water contents of prepared films in terms of PMAm11 nanoparticles contents. (b) Water contents of prepared films in terms of MMA contents (mole) of nano-sized PMMA-*co*-AAm. (c) Water contents of prepared films added with different particle size of PMAm41.

Table 3 lists DS and *S* values of films added with PMMA-*co*-AAm prepared at the different mole ratio of MMA and AAm. DS value of the films increased with the increase in the MMA mole ratio whereas *S* value decreased. These results indicate that the water resistance of the films has improved with the increase of MMA content. However, in the case of films added with PMMA nanoparticles, the degree of water resistance was weakened compared to the other films added with copolymer nanoparticles due to low DS value and high *S* value. Probably because the elastic collision of particle intensified and the hydrophobic property of PMMA particles caused phase separations in the composites, a poor dispersion of the nanoparticles is formed in the starch/PVA composites.

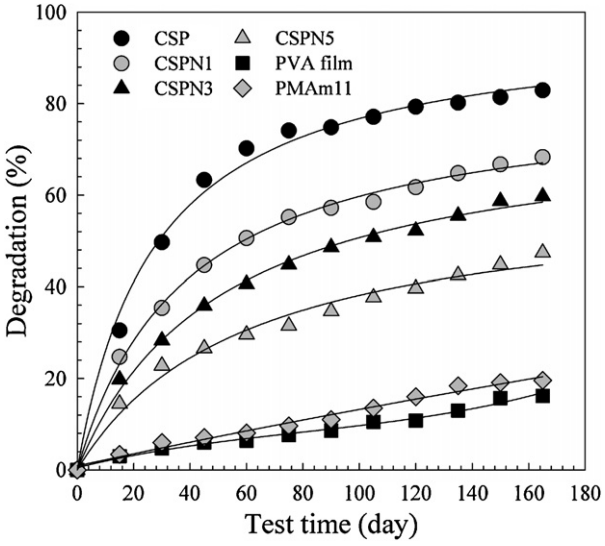

Fig. 8. Biodegradation of films with/without PMAm11 in the soil burial test.

3.4. Water vapor absorption

One of the major defects of starch-based material is its water absorption tendency, and improvement in water resistance is an important issue. Therefore, this study examined the water contents of prepared the films with nano-sized PMMA-*co*-AAm contents, MMA mole ratio of PMMA-*co*-AAm, and particle size of PMMA-*co*-AAm, and the results are shown in Fig. 7. It can be found that the water vapor absorption of the films decreased with the increase of PMMA-*co*-AAm contents and MMA mole ratio of PMMA-*co*-AAm, except for films prepared by adding different particle size PMMA-*co*-AAm. The reason of the increase of water content for films added PMMA-*co*-AAm particles with the difference particle sizes was because of the formation of voids and the agglomeration between copolymer particles (see Fig. 6).

3.5. Soil burial degradation

The biodegradation of the soil burial is an outside experimental method, and tenders a realistic environment that temperature, humidity, and sort of soil and amount of microorganisms are at least controlled and changed with season. All the films had the same size and shape to prevent the effect of the shape of films on its biodegradation (Yang, Yoon, & Kim, 2005).

As shown in Fig. 8, the degree of biodegradation of the films was investigated by weight loss of the films with time. In case of the starch/PVA film without PMMA-*co*-AAm nanoparticles, a rapid biodegradation occurred in the initial 60 days, followed by a slow degradation until the end of the test. The starch/PVA composite films added PMMA-*co*-AAm nanoparticles degraded rapidly in the initial 80 days, and a gradual degradation took place until the end of the experiment although the degree of biodegradation had the difference with increasing PMMA-*co*-AAm nanoparticles contents. In contrast, the PVA film and PMAm11 revealed resistance against soil burial biodegradation.

4. Conclusions

Starch/PVA composite films were successfully synthesized by using nano-sized poly(methyl methacrylate-*co*-acrylamide) (PMMA-*co*-AAm) particles, which were prepared by using emulsion polymerization and glycerol (GL), xylitol (XL), and citric acid (CA) as additives. In order to investigate the effect of the change of MMA mole ratio with hydrophobic of PMMA-*co*-AAm and the particle sizes of PMMA-*co*-AAm for the films, copolymer nanoparticles with the different mole ratio of MMA and AAm were also prepared. The conversion of PMMA-*co*-AAm using TGA was about 99.0%. The surface and shape verified by SEM were mainly smooth and had a regular spherical shape. In addition, PMMA-*co*-AAm particles controlled by the change of initiator concentration were about 60, 100, 150, and 200 nm, respectively.

It was found from the results of the physical properties that TS and DS values increased with increasing PMMA-*co*-AM nanoparticles contents, whereas %E, *S*, and water vapor absorption decreased. Although each film had different additives, the physical properties of each film were improved by adding PMMA-*co*-AM nanoparticles. Especially, the low *S* values and water vapor absorption indicate that water resistance of films had improved. It was also noted from the changing effect of MMA mole ratio of PMMA-*co*-AAm that TS and DS slightly increased with increasing MMA mole ratio with hydrophobic property, whereas %E, *S*, and water vapor absorption decreased. However, in the case of films where only the hydrophobic PMMA nanoparticle was added, the physical properties deteriorated due to the absence of the functional group which can combine between starch, PVA and additives with hydrophilic properties. On the other hand, the effect of particle size on the films can be classified into two parts: (1) in the case of the films added PMMA-*co*-AAm particles with less than 150 nm, the physical properties were relatively constant and (2) in the case of the films added PMMA-*co*-AAm particles with more than 150 nm, however, the properties have tended to be weakened due to the agglomerations and phase separation between the components of films and copolymer particles.

The results of the soil burial biodegradation indicated that the starch/PVA composite films added PMMA-*co*-AAm nanoparticles degraded rapidly in the initial 80 days, and a gradual degradation took place about 45–65% for 165 days until the end of the experiment although the degree of biodegradation was different with increasing PMMA-*co*-AAm nanoparticles content.

Acknowledgment

This research was supported by Basic Science Research Program Through the National Research Foundation (NRF) funded by the Ministry of Education, Science and Technology (Grant No. 2011-0002766).

References

Ahamed, N. T., Singhal, R. S., Kulkarni, P. R., Kale, D. D., & Pal, M. (1996). Studies on Chenopodium quinoa and Amaranthus paniculatas starch as biodegradable fillers in LDPE films. *Carbohydrate Polymers*, *31*, 157–160.

Anglès, N. M., & Dufresne, A. (2000). Plasticized starch/tunicin whiskers nanocomposites. 1. Structural analysis. *Macromolecules*, *33*, 8344–8353.

Avella, M., De Vlieger, J. J., Errico, M. E., Fischer, S., Vacca, P., & Volpe, M. G. (2005). Biodegradable starch/clay nanocomposite films for food packaging applications. *Food Chemistry*, *93*, 467–474.

Azeredo, H. M. C. (2009). Nanocomposites for food packaging applications. *Food Research International*, *42*, 1240–1253.

Cabedo, L., Gimenez, E., Lagaron, J. M., Gavara, R., & Saura, J. J. (2004). Development of EVOH–kaolinite nanocomposites. *Polymer*, *45*, 5233–5238.

Chang, J. H., An, Y. U., & Sur, G. S. (2003). Poly(lactic acid) nanocomposites with various organoclays. I. Thermomechanical properties, morphology, and gas permeability. *Journal of Polymer Science: Part B: Polymer Physics*, *41*, 94–103.

Chivrac, F., Pollett, E., & Schmutz, M. (2008). New approach to elaborate exfoliated starch-based nanobiocomposites. *Biomacromolecules*, *9*, 896–900.

Cyras, V. P., Manfredi, L. B., Ton-That, M. T., & Vázquez, A. (2008). Physical and mechanical properties of thermoplastic starch/montmorillonite nanocomposite films. *Carbohydrate Polymers*, *73*, 55–63.

Dean, K., Yu, L., & Wu, D. Y. (2007). Preparation and characterization of melt-extruded thermoplastic starch/clay nanocomposites. *Composites Science Technology*, *67*, 413–421.

Guana, J., Eskridgeb, K. M., & Hannaa, M. A. (2005). Acetylated starch–polylactic acid loose-fill packaging materials. *Industrial Crops and Products*, *22*, 109–123.

Huneault, M. A., & Li, H. (2007). Morphology and properties of compatibilized polylactide/thermoplastic starch blends. *Polymer*, *48*, 270–280.

Ishiaku, U. S., Pang, K. W., Lee, W. S., & Ishak, Z. A. M. (2002). Mechanical properties and enzymic degradation of thermoplastic and granular sago starch filled poly(ε-carprolactone). *European Polymer Journal*, *38*, 393–401.

Jordan, J., Jacob, K. I., Tannenbaum, R., Sharaf, M. A., & Jasiuk, I. (2005). Experimental trends in polymer nanocomposites—A review. *Material Science Engineering A*, *393*, 1–11.

Khan, M. A., Bhattacharia, S. K., Kader, M. A., & Bahari, K. (2006). Preparation and characterization of ultra violet (UV) radiation cured bio-degradable films of sago starch/PVA blend. *Carbohydrate Polymers*, *63*, 500–506.

Koenig, M. F., & Huang, S. J. (1995). Biodegradable blends and composites of polycaprolactone and starch derivatives. *Polymer*, *36*, 1877–1882.

Lee, S. Y., Chen, H., & Hannaa, M. A. (2008). Preparation and characterization of tapioca starch–poly(lactic acid) nanocomposite foams by melt intercalation based on clay type. *Industrial Crops and Products*, *28*, 95–106.

Liao, H. T., & Wu, C. S. (2009). Preparation and characterization of ternary blends composed of polylactide, poly(ε-caprolactone) and starch. *Material Science Engineering A*, *515*, 207–214.

Ma, X., Jian, R., Chang, P. R., & Yu, J. (2008). Fabrication and characterization of citric acid-modified starch nanoparticles/plasticized-starch composites. *Biomacromolecules*, *9*, 3314–3320.

Mathew, A. P., & Dufresne, A. (2002). Plasticized waxy maize starch: Effect of polyols and relative humidity on material properties. *Biomacromolecules*, *3*, 1101–1108.

Mathew, S., Brahmakumar, M., & Abraham, T. E. (2006). Microstructural imaging and characterization of the mechanical, chemical, thermal, and swelling properties of starch–chitosan blend films. *Biopolymers*, *82*, 176–187.

Ogata, N., Jimenez, G., Kawai, H., & Ogihara, T. (1997). Structure and thermal/mechanical properties of poly(L-lactide)-clay blend. *Journal of Polymer Science: Part B: Polymer Physics*, *35*, 389–396.

Park, H. M., Lee, W. K., Park, C. Y., Cho, W. J., & Ha, C. S. (2003). Environmentally friendly polymer hybrids. Part I: Mechanical, thermal, and barrier properties of thermoplastic starch/clay nanocomposites. *Journal of Material Science*, *38*, 909–915.

Pluta, M., Galeski, A., Alexandre, M., Paul, M. A., & Dubois, P. (2002). Polylactide/montmorillonite nanocomposites and microcomposites prepared by melt blending: Structure and some physical properties. *Journal of Applied Polymer Science*, *86*, 1497–1506.

Psomiadou, E., Arvanitoyannis, I., Biliaderis, C. G., Ogawa, H., & Kawasaki, N. (1997). Biodegradable films made from low density polyethylene (LDPE), wheat starch and soluble starch for food packaging applications. Part 2. *Carbohydrate Polymers*, *33*, 227–242.

Ren, J., Fu, H., Ren, T., & Yuan, W. (2009). Preparation, characterization and properties of binary and ternary blends with thermoplastic starch, poly(lactic acid) and poly(butylene adipate-co-terephthalate). *Carbohydrate Polymers*, *77*, 576–582.

Rhim, J. W., Hong, S. I., & Ha, C. S. (2009). Tensile, water vapor barrier and antimicrobial properties of PLA/nanoclay composite films. *LWT-Food Science Technology*, *42*, 612–617.

Tang, H., Xiong, H., Tang, S., & Zou, P. (2009). A starch-based biodegradable film modified by nano silicon dioxide. *Journal of Applied Polymer Science*, *113*, 34–40.

Tang, S. W., Zou, P., Xiong, H. G., & Tang, H. L. (2008). Comparative study of pasting and thermal transition characteristics of osmotic pressure and heat–moisture treated corn starch. *Carbohydrate Polymers*, *72*, 521–526.

Thakore, I. M., Desai, S., Sarawade, B. D., & Devi, S. (2001). Studies on biodegradability, morphology and thermomechanical properties of LDPE/modified starch blends. *European Polymer Journal*, *37*, 151–160.

Veregin, R. P. N., Odell, P. G., Michalak, L. M., & Georges, M. K. (1996). The pivotal role of excess nitroxide radical in living free radical polymerizations with narrow polydispersity. *Macromolecules*, *29*, 2746–2754.

Vert, M., Santos, I. D., Ponsart, S., Alauzet, N., Morgat, J. L., Coudance, J., et al. (2002). Degradable polymers in a living environment: Where do you end up? *Polymer International*, *51*, 840–844.

Xiong, H. G., Tang, S. W., Tang, H. L., & Zou, P. (2008). The structure and properties of a starch-based biodegradable film. *Carbohydrate Polymers*, *71*, 263–268.

Yang, H. S., Yoon, J. S., & Kim, M. N. (2005). Dependence of biodegradability of plastics in compost on the shape of specimens. *Polymer Degradation and Stability*, *87*, 131–135.

Yoon, S. D., Chough, S. H., & Park, H. R. (2006). Effects of additives with different functional groups on the physical properties of starch/PVA blend film. *Journal of Applied Polymer Science*, *100*, 3733–3740.

Yoon, S. D., Chough, S. H., & Park, H. R. (2007). Preparation of resistant starch/poly(vinyl alcohol) blend films with added plasticizer and crosslinking agents. *Journal of Applied Polymer Science*, *106*, 2485–2493.

Yu, Y. H., Lin, C. Y., Yeh, J. M., & Lin, W. H. (2003). Preparation and properties of poly(vinyl alcohol)–clay nanocomposite materials. *Polymer*, *44*, 3553–3560.

Yun, Y. H., & Yoon, S. D. (2010). Effect of amylose contents of starches on physical properties and biodegradability of starch/PVA-blended films. *Polymer Bulletin*, *64*, 553–568.

Yun, Y. H., Wee, Y. J., Byun, H. S., & Yoon, S. D. (2008). Biodegradability of chemically modified starch (RS4)/PVA blend films. Part 2. *Journal of Polymers and the Environment*, *16*, 12–18.

Zhai, M., Yoshii, F., & Kume, T. (2003). Radiation modification of starch-based plastic sheets. *Carbohydrate Polymers*, *52*, 311–317.